Research paper submitted to *Atmospheric Environment*

Ms. Ref. No.: ATMENV-D-08-01147

Title

Reactivity between $PbSO_4$ and $CaCO_3$ Particles Relevant to the Modification of Mineral Particles and Chemical Forms of Pb in Particles Sampled at Two Remote Sites during an Asian Dust Event

Authors

Takahiro ISHIZAKA[1], Susumu TOHNO[1*], Chang-Jin MA[2], Atsushi MORIKAWA[1], Masaki TAKAOKA[3], Fumitaka NISHIYAMA[4], and Kouhei YAMAMOTO[1]

Affiliations

[1] Graduate School of Energy Science, Kyoto University, Uji, Kyoto 611-0011, Japan

[2] Fukuoka Women's University, Higashi-ku, Fukuoka 813-8529, Japan

[3] Graduate School of Engineering, Kyoto University, Nishikyo-ku, Kyoto 615-8540, Japan

[4] Graduate School of Engineering, Hiroshima University, Higashi-Hiroshima, Hiroshima 739-8527, Japan

*Corresponding author

E-mail: tohno@energy.kyoto-u.ac.jp

Tel.: +81-774-38-4408

Fax: +81-774-38-4411

Abstract

During the transboundary transport of anthropogenic heavy metals by mineral particles providing reaction sites, the divalent metal salt $PbSO_4$ can be converted to $PbCO_3$ in the presence of water. We carried out laboratory experiments to study the transformation process under various conditions by incorporating test particles comprising $CaCO_3$ of a particulate mineral component, $PbSO_4$, and NaCl. After the immersion of $PbSO_4$ particles in contact with $CaCO_3$ particles in a water droplet, the conversion of $PbSO_4$ into $PbCO_3$ was confirmed by the change in morphology of the original particles to stick or needle form; the percentages of the chemical forms relative to the total Pb were determined by X-ray absorption near edge structure (XANES) analysis. Approximately 60–80% of $PbSO_4$ was converted to $PbCO_3$ after 24 h. A small amount of stick particles was detected when NaCl particles attached to $PbSO_4$/$CaCO_3$ particles were exposed to air with a relative humidity (RH) of 80–90% for 24 h. XANES measurements of the samples revealed that the molar percentage of $PbCO_3$ relative to the total Pb content was 4%.

Field experiments were also conducted to determine the chemical forms of the Pb particles during the *Kosa* (Asian dust storm) event. Samples were collected from two remote sites in Japan and Korea. The mass size distribution of Pb aerosols collected in Japan was bimodal with two peaks in the coarse mode; the enrichment factor of Pb suggested that its source was anthropogenic. Pb L3 edge XANES measurements of both samples indicated that they had similar shapes. These measurements also indicated that the major Pb components for the samples collected in Japan were PbO, $PbSO_4$ $PbCl_2$, and $PbCO_3$, with molar percentages of 44%, 30%, 21%, and 5%, respectively. No significant differences were found between the component ratios of the samples collected in Japan and Korea, suggesting that definite transformation did not occur during the transport of the *Kosa* particles from Korea to Japan. On the basis of these observations, we postulate that the transformation process either occurred mainly before the particles arrived at Korea or did not take place after the particles left continental Asia.

Key Words: Mineral dust; XANES; Transformation; Deliquescent particles; $PbSO_4$; $PbCO_3$

1. Introduction

Mineral dust originating from arid and semi-arid regions has local as well as global effects. For example, mineral aerosols influence radiative transfer through the direct absorption and scattering of solar and terrestrial radiation; they also have indirect effects through their changing the optical properties and lifetime of clouds as cloud condensation nuclei (CCN). Long-range transported mineral aerosols can affect remote marine ecosystems as a source of biogeochemically important elements by providing reaction sites and serving as carriers for various condensed species (Hand et al., 2004). Airborne mineral dust also plays an important role in chemical reactions in the atmosphere, such as serving as a reaction surface for the photochemical oxidation cycles in the troposphere. In addition, elevated concentrations of mineral dust in the respiratory size range can adversely affect human health.

Mineral dust has the potential to undergo various reactions with anthropogenic air pollutants such as SO_2, HNO_3, and heavy metal particulates during long-range transport. Laboratory experiments (Goodman et al., 2000; Krueger et al., 2003; Krueger et al., 2004; Morikawa et al., 2007) have been conducted to study the reactivity of acidic gases and the particulate mineral components of $CaCO_3$. In addition, field measurements (Nishikawa et al., 1991; Zhang et al., 1999; Trochkine et al., 2003; Morikawa et al., 2006) have been carried out to understand the modification of *Kosa* particles in terms of SO_4^{2-} and NO_3^- formation. Clay minerals are the most important absorbents/sorbents of metals in natural systems (Sparks et al., 2005). The interaction between divalent metallic ions (Cd^{2+}, Pb^{2+}, Zn^{2+}, etc.) and $CaCO_3$ that occurs in aqueous solutions has been studied in order to decontaminate or fix toxic heavy metal ions in natural and waste water (El-Korashy et al., 2003) and to evaluate their chemical mobility in the geosphere and biosphere (Godelitsas et al., 2003). However, very few studies have been performed that explain the reactivity of mineral aerosols and airborne metal salt particles.

The long-range transport of trace metal aerosols has been observed in southern China (Lee et al., 2007) and elevated concentrations of heavy metals have been observed in Korea (Han et al., 2004) and

Japan (Hioki et al., 2006) during *Kosa* or Asian dust storm events. Sun et al. (2005) suggested that a mixing of mineral aerosols with pollution aerosols occurs along the path between the desert areas and Beijing. Tohno et al. (2006) observed individual *Kosa* particles collected at a coastal background site in Japan using a synchrotron radiation (SR) X-ray microprobe and found that they were remarkably enriched with trace metals. They also identified the presence of mineral components and heavy metals such as Ni and Pb in a single particle. The transboundary transport of anthropogenic trace elements by mineral aerosols has also been reported in the eastern Mediterranean region (Erel et al., 2006) and New Zealand (Marx et al., 2008). These observations suggest that natural mineral aerosols and anthropogenic metal particles exhibit simultaneous mixing and transportation along with mutual interaction.

In China, coal accounts for approximately 60% of the primary energy demand (IEA, 2007) and coal combustion is one of the major emission sources of rare metal particles. Soil dust and combusted coal are considered to be the major primary sources of metal aerosols in Beijing (Okuda et al., 2004). Furthermore, in order to fuel its astounding economic growth, China's energy requirements are expected to grow continuously; because of this, there is growing concern regarding the possible increase in the transboundary transport of metallic aerosols. $PbSO_4$ is one of the main constituents of a majority of Pb aerosols resulting from coal combustion (Gieré et al., 2006) and Pb smelters (Sobanska et al., 1999); $PbSO_4$ reacts with $CaCO_3$ in the presence of water. Falgayrac et al. (2006) employed Raman microspectrometry to determine the reaction products of $PbSO_4$ particles deposited on the surface of calcite ($CaCO_3$) after immersion in a water droplet; he identified $Pb_3(CO_3)_2(OH)_2$, $PbCO_3$ and $CaSO_4 \cdot 2H_2O$ on the calcite surface. Their formation can be expressed by the following equations:

$$3Pb^{2+} + 2CO_3^{2-} + 2H_2O \rightarrow Pb_3(CO_3)_2(OH)_2\,(s) + 2H^+ \quad (1)$$

$$Pb^{2+} + CO_3^{2-} \rightarrow PbCO_3\,(s) \quad (2)$$

Water is indispensable for the formation of $PbCO_3$ in reactions (1) and (2). After drying, $CaSO_4 \cdot 2H_2O$ (gypsum) crystallization occurs on the particle surface.

$$Ca^{2+} + SO_4^{2-} + 2H_2O \rightarrow CaSO_4 \cdot 2H_2O \quad (3)$$

$PbCO_3$ is water-insoluble and remains in the environment. In addition, Barltrop and Meek (1975) reported that $PbCO_3$ showed the highest absorption of dietary lead compounds for rats. Therefore, the transformation of $PbSO_4$ to $PbCO_3$ is an environmentally important process

Airborne Asian dust is often transported until Japan through an extratropical cyclone and then arrives over Japan with the passage of a cold front (Bates et al., 2004). During the atmospheric transport, dust particles are expelled in the form of CCN (Ma et al., 2004b) or internally mixed particles are formed after the evaporation of cloud droplets accompanied with aqueous reactions. Alternatively, the presence of an internal mixture of mineral dust and sea salts (Ma et al., 2004a; Zhang et al., 2004) can provide reaction sites under conditions of high humidity. Thus, the above-mentioned cloud process or mixing of sea salts with mineral dust can contribute to the formation of $PbCO_3$ particles during long-range transport.

In this paper, we report on the results of a laboratory experiment involving the reactions of $CaCO_3$ microparticles incorporated with $PbSO_4$ microparticles under the following three conditions: (1) in a water droplet, (2) highly humid atmosphere, and (3) attachment of deliquescent particles under a highly humid atmosphere. X-ray absorption near edge structure (XANES) spectrometry was used to determine the chemical forms of Pb in the particles and their molar percentages. Furthermore, we carried out field measurements to determine the chemical states of Pb in the aerosols at two remote sites in Japan and Korea during the *Kosa* event and study the changes in the chemical forms using XANES.

2. Experiments

2.1. Laboratory experiment

2.1.1. Sample preparation

A fluidized bed aerosol generator (TSI, model 3400) was used to generate aerosols from $CaCO_3$

powders (>99.5% purity, Nacalai Tesque). The $CaCO_3$ particles were collected on a supported polytetrafluoroethylene (PTFE) filter (diameter: 47 mm; pore size: 1.0 μm, ADVANTEC, J100A047A) inserted into an in-line filter holder. $PbSO_4$ aerosols were generated from milled $PbSO_4$ powders (>99.5% purity, Nacalai Tesque) dispersed in ethanol by a jet nebulizer (Origin Medical Instruments, JN-60). A $PM_{2.5}$ impactor was used to collect the dry $PbSO_4$ aerosols onto the filter where $CaCO_3$ particles were already deposited. In this manner, we prepared the reaction sample—i.e., $PbSO_4$ particles attached the $CaCO_3$ particles—hereafter denoted as SP-I. A supported PTFE filter (ADVANTEC, J100A025A) with a diameter of 25 mm was used to prepare the samples denoted as SP-II for chemical analysis. The deposited mass of each particle was estimated by weighing the filter on a microbalance (Sartorius, M5-F) before and after collection.

Mass size distributions for both aerosols were determined using an 8-stage Andersen sampler (Koritsu). The cut-off diameters (at 50% collection efficiency) of the sampler, operating at 28.3 $L \cdot min^{-1}$, were 11, 7.0, 4.7, 3.3, 2.1, 1.1, 0.65, and 0.43 μm in aerodynamic diameters at each stage. A polyethylene foil (thickness: 30 μm), placed on each stage, was used as an impaction substrate and a Nuclepore filter (pore size: 0.4 μm, diameter: 80 mm) was employed as the backup filter.

NaCl aerosols were produced by nebulizing a 0.01 M NaCl (>99.9% purity, Wako) solution using the jet nebulizer and then dried with a diffusion dryer. The dry NaCl aerosols were deposited onto the above-mentioned SP-I and SP-II samples (hereafter denoted as SP-III).

2.1.2. Methods of analysis

The samples produced with the procedures above were subjected to Pt–Pd coating for approximately 1 min by an ion sputter coater (Hitachi, E-102); they were then examined under a Hitachi S-3000H scanning electron microscope (SEM) equipped with an energy dispersive X-ray spectrometer (EDAX, DX-4).

Pb L3 edge XANES spectra of the samples were measured at the beamline BL14B2 equipped with a

double-crystal Si (111) monochromator in SPring-8 (Super Photon ring 8GeV), a third-generation synchrotron radiation facility in Hyogo, Japan. The spectra were collected in the transmission mode using an ionization chamber over the energy range 12780–13280 eV. The sample filter was folded in order to enhance the particle density. The spectra of two reference materials ($PbSO_4$ and $PbCO_3$) were also measured and the linear combination fit (LCF) technique, in which spectra of the two known reference species are fitted to the spectrum of the unknown sample, was used to determine the molar percentage of each compound in the sample (Roberts et al., 2003). The commercially available software REX 2000 ver. 2.3 (Taguchi et al., 2005) was used to fit the spectra of the two reference species to that of the sample. The partial concentration was refined for each reference spectrum in the LCF of XANES. The residual value (R) was calculated using the following equation.

$$R = \frac{\sum\left(XANES_{measured} - XANES_{calculated}\right)^2}{\sum\left(XANES_{measured}\right)^2} \quad (4)$$

The calculated R value was used to evaluate the LCF of the sample spectra.

2.1.3. Experimental conditions

The experiments were carried out in a humid air flow chamber under the following conditions: (1) treatment of the samples with drops of pure water (1 mL of pure water for SP-I and 100 μL of pure water for SP-II), using a micropipette to immerse the particles in water; and (2) exposure of the samples (SP-I, SP-II, and SP-III) to highly humid air. Table 1 shows the samples and their respective reaction times during the XANES measurements. The sample type is indicated by the abbreviations of A1, A2, B1, B2, and D. A bulk sample of the mixture of $CaCO_3$ and $PbSO_4$ powders, which was immersed in 1 mL of pure water for 3 days, was prepared to serve as the reference sample.

2.2. *Kosa* measurements

2.2.1. Sampling method

In order to determine the chemical forms of Pb in the *Kosa* samples and study the changes in the forms during their long-range transport, simultaneous aerosol samplings were carried out at two remote sites (Yasaka, Japan and Byunsan, Korea) over which air masses propagate during *Kosa* events. Yasaka (35.41°N, 135.09°E, altitude: 80 m), which once housed a national acid rain monitoring station, is a rural site located in the center of the Tango peninsula with no major anthropogenic sources located within its vicinity. During the spring, Yasaka is directly exposed to an influx of air masses from the Chinese continent and Korean peninsula. Byunsan (35.37°N, 126.27°E, altitude: 30 m) is a coastal site without any major anthropogenic sources located nearby.

At each site, *Kosa* samples were collected onto a 203×254 mm Teflon filter (ADVANTEC, PF040) using a high-volume sampler (Kimoto, 120F) at a flow rate of 1 $m^3 \cdot min^{-1}$. Sampling periods were from March 31 to April 1, 2007 at Byunsan (321 m^3 of total air volume) and from April 1 to April 2, 2007 at Yasaka (1773 m^3 of total air volume). The sampler at Yasaka was equipped with a PM_{10} cyclone while the one at Byunsan was not.

Size-segregated aerosol particles were collected onto polyethylene foils using an 8-stage Andersen sampler (Koritsu) at Byunsan (9.1 m^3 of total air volume) and a 12-stage low-pressure type impactor (Tokyo-Dylec, LP-20) at Yasaka (40.7 m^3 of total air volume). A Nuclepore filter (pore size: 0.4 μm, diameter: 80 mm) was used as a backup filter. The aerodynamic cut-off diameters (at 50% collection efficiency) of the latter sampler were 11, 7.8, 5.2, 3.5, 2.1, 1.2, 0.69, 0.49, 0.6, 0.2, 0.12, and 0.06 μm when operated at 23.3 $L \cdot min^{-1}$. The onset of the *Kosa* event was confirmed by an abrupt increase in the number concentration of coarse particles with diameters greater than 5 μm; this was measured by an optical particle counter (RION, KC-01D), as shown in Fig. 1. Figure 1 illustrates the time lag between the arrival of *Kosa* with the elevated increase in concentration of coarse particles (0:00 a.m. on April 1) and the arrival of anthropogenic polluted air parcels with that of only fine particles (6:00 a.m. on March 31). Since our sampling began after the arrival of *Kosa* particles, the effect of anthropogenic polluted air

parcels was not included. The weather was cloudy throughout the duration of sampling and Fig. 1 shows highly humid conditions during the sampling period at Yasaka.

The backward trajectory analysis, shown in Fig. 2, suggests that *Kosa* particles arriving from the arid regions of China reached Yasaka after having passed over Beijing, the Yellow Sea, Korea, and the Sea of Japan.

2.2.2. Analytical methods

The *Kosa* particles collected by the high-volume sampler onto a filter were transferred into a polyethylene bag using a spatula and analyzed by XANES. Pb L3 edge XANES spectra of the samples were measured at the beamline BL14B2 in SPring-8 and the spectra were collected in the fluorescence mode using a 19-element solid-state detector (SSD).

The foils and the filters were dried in a desiccator before and after particle collection for approximately 24 h; the total mass concentrations of the aerosols were then determined by weighing the total mass deposited at each stage using the microbalance. The size-segregated aerosol samples were cut into several pieces and subjected to ultrasonification in pure water for 20 min and then filtered through Nuclepore filters (pore size: 0.2 μm). Consequently, the water-soluble components were separated in the form of filtrates and the water-insoluble components in the form of residues. The elemental mass concentrations of the insoluble components in the size-segregated particles collected at Yasaka were determined by the particle induced X-ray emission (PIXE) method. The PIXE analysis was carried out using an ion beam analysis instrument at the radiation research facility of Hiroshima University. The beam size diameter and accelerating voltage of the irradiated proton beam were 7 mm and 2.0 MeV, respectively. In order to enable the analysis of lighter elements, the accelerating voltage of the beam was reduced to 1.25 MeV. The analytical elements were Na, Mg, Al, Si, P, S, Cl, K, Ca, Ti, V, Cr, Mn, Fe, Ni, Cu, Zn, Sr, and Pb. The mass concentration for each element was determined by analyzing energy-dispersive X-ray spectra using the GUPIX software (Maxwell et al., 1995). To

determine the mass concentrations of water-soluble Pb in the size-segregated aerosols, 100 μL of the filtrate for each sample was dropped onto a polycarbonate film and the film was subjected to PIXE analysis. However, lead concentrations were below the detection limit of the PIXE method due to the small sample amounts.

Ion chromatography (IC, Shimadzu HIC-10A) was used to determine the equivalent concentrations of the nine ionic components—Na^+, NH_4^+, K^+, Mg^{2+}, Ca^{2+}, Cl^-, NO_2^-, NO_3^-, and SO_4^{2-}—in the water-soluble components.

3. Results and Discussion

3.1. Laboratory experiment

3.1.1. Morphological change in the particles

The generated $CaCO_3$ and $PbSO_4$ particles were found to have unimodal mass size distributions; the modes were several micrometers in aerodynamic diameter, as illustrated in Fig. 3. The mass size distribution of $CaCO_3$ particles exhibited a peak at 10 μm; however, scanning electron micrographs of the $CaCO_3$ particles showed that the peak was from an aggregate of particles from the first peak. The crystal form of $PbSO_4$ (anglesite) and $CaCO_3$ (calcite) is known to be orthorhombic and the morphologies of the $PbSO_4$ and $CaCO_3$ particles in this study were cluster and cubic forms, respectively, as shown in Fig. 4. The size distribution of the NaCl particles was unimodal with a peak at ~1 μm.

Before initiating our experiments, we established that the immersion of $CaCO_3$ or $PbSO_4$ particles in water did not cause any change in their morphologies. Figure 4 shows the morphology of SP-I after immersion in a water droplet for 3 h and subsequent drying (Run 1); newly formed stick crystals were found after the reaction. Furthermore, exposure of SP-I to a highly humid atmosphere (Run 2) did not result in morphological changes either. However, exposure of SP-III to air with a high RH of 80–90%

(Run 3) resulted in the formation of stick crystals and the presence of Na and Cl near the crystals—as shown in Fig. 5—was confirmed. Since the deliquescent relative humidity (DRH) of NaCl is 75%, the presence of Na and Cl near the crystals suggests that the reaction between $CaCO_3$ and $PbSO_4$ occurred through the NaCl solution droplet. Falgayrac et al. (2006) demonstrated dramatic changes in the morphology of the $PbSO_4$ aggregate on the $CaCO_3$ surface after immersion in a water droplet for 1–10 min. This dramatic change was due to the formation of hexagonal plates of precipitated hydrocerussite ($Pb_3(CO_3)_2(OH)_2$) and, depending upon the pH of the water droplet in which the sample is immersed, stick-shaped crystals of cerussite ($PbCO_3$). Therefore, the stick crystals formed in our experiments were assumed to be composed of only cerussite and not hydrocerussite due to the long reaction time of our experiment (Godelitsas et al., 2003).

The changes in the morphology of the sample particles after our experiments were estimated from the aspect ratio, which is defined as the ratio of the longest and shortest dimensions of a particle. Figure 6 shows the distributions of the aspect ratios for the above three samples in Runs 1–3. The aspect ratios of ~200 particles in each sample were determined.

The mean aspect ratios in Runs 1, 2, and 3 were 2.55, 1.56, and 1.5, respectively. The aspect ratio distribution of the sample particles before the runs was nearly the same as that in Run 2. For Runs 2 and 3, the aspect ratio distributions showed a peak at ~1.6, whereas the aspect ratio in the case of Run 1 showed a peak at ~2.8 and shifted to a right tail distribution. Various ratios of stick crystals were formed through the conversion of particles in the presence of water. In addition to the primary peak at ~1.5, a small peak at ~8 was found for SP-III, which suggests that a faint transformation was caused by slight contact of the mineral and $PbSO_4$ particles with NaCl crystals.

3.1.2. XAFS analysis

Figure 7 illustrates the XANES spectroscopy measurements at the Pb L3 edge of the samples and the reference compounds of $PbSO_4$ and $PbCO_3$. The spectra of both reference materials were found to be

similar, with peaks at 13045 and 13050 eV for $PbSO_4$ and $PbCO_3$, respectively. A comparison of the XANES spectra of the samples with those of the reference compounds revealed that $PbCO_3$ was the primary Pb component in samples A1, A2 and D, while $PbSO_4$ was the main component in samples B1 and B2.

Table 2 shows the molar percentages of two Pb compounds relative to the total Pb content by applying the LCF technique to the XANES spectra of the samples. More than 90% of $PbSO_4$ in the bulk samples was found to be converted to $PbCO_3$ after interaction with $CaCO_3$ in aqueous phase; this conversion rate in the microparticles immersed in water droplets (samples A1 and A2) ranged between 60–90%. In samples B1, B2, C1, and C2, $PbSO_4$ was the major constituent and the conversion rate was only ~4%. Since reactions (1) and (2) proceed in the aqueous phase, $PbCO_3$ barely formed in a highly humid atmosphere without any aqueous phase. Under conditions of high humidity, SP-III deliquesced and the morphological analysis confirmed the formation of stick or needle crystals of $PbCO_3$. However, only a small quantity of $PbCO_3$ was formed and hardly any difference in the conversion rates for samples B and C was found. Above the DRH for NaCl, aqueous droplets for the reaction sites were formed but the droplets needed contact with both $CaCO_3$ and $PbSO_4$ particles. In our samples, the volume ratios of $PbSO_4$ to NaCl and to $CaCO_3$ ranged from 4 to 15 and 44 to 140, respectively. This implies that partial contact of NaCl droplets with both $PbSO_4$ and $CaCO_3$ particles led to the lower level of $PbCO_3$ formation.

3.2. Chemical characteristics of the *Kosa* samples

3.2.1. Mass size distribution

Figure 8 shows the total mass size distributions of aerosols sampled during the *Kosa* event at Yasaka and Byunsan. The total mass concentrations at Yasaka and Byunsan were 358 $\mu g \cdot m^{-3}$ and 489 $\mu g \cdot m^{-3}$, respectively. An extremely strong *Kosa* event was observed over a large region of western Japan, and

the total mass concentration at Yasaka was roughly 20–30 times higher than that during non-*Kosa* periods. Particles with diameters larger than 11 μm account for 34% of the total mass concentration at Byunsan but account for only 9% at Yasaka; this difference can be attributed to not only the gravitational settling of large particles during transport but also the sampling of dust particles from different parts of the whole dust plume in Korea and Japan. At Yasaka, water-insoluble components account for 89% of the total mass concentration.

Figure 9 exhibits the size distributions of Pb and Si in the water-insoluble components at Yasaka. The total mass concentrations of Si and Pb were 57.1 $\mu g \cdot m^{-3}$ and 178 $ng \cdot m^{-3}$, respectively. Si, which is a major component of mineral dust, exhibited a unimodal size distribution with its peak occurring in coarse mode and its distribution similar to that of the total mass concentration. Water-insoluble Pb present in the samples showed a bimodal distribution with two peaks in the coarse mode, and its distribution profile is dissimilar to that of Si. The size distribution of Pb in urban areas has been characterized by the unimodal mode with a peak occurring in the sub-micron range (Singh et al., 2002; Sun et al., 2006; Karanasiou et al., 2007) while a bimodal distribution with a peak in the fine mode has also been observed (Singh et al., 2002; Pakkanen et al., 2003; Sun et al., 2006). A greater occurrence of the fine mode when compared to that of the coarse mode in the size distribution of Pb was also exhibited in the samples collected during the *Kosa* events (Mori et al., 2003; Hioki et al., 2006). Our results differ remarkably from those of previous studies. Sun et al. (2005) reported the shift of a major part of Pb from fine fractions in winter to coarse fractions in spring in Beijing; the mixing of transported dust with anthropogenic pollutants along the path could be a probable cause for this shift. Our size-segregated samples contained only the water-insoluble components of Pb because water-soluble components were below the detection limit; samples analyzed in the previous studies contained both water-insoluble and water-soluble components and their fractions are unknown. Funasaka et al. (2008) demonstrated that the water-soluble fraction of Pb in atmospheric aerosols collected with a high volume sampler at urban sites in Japan ranged 0.2–20% of total Pb and 14–19% in the samples collected in the

month of March, indicating that the samples collected in March were likely to contain Asian dust. The difference in the size distributions between our results and those of previous studies may be attributed to the presence or absence of the water-soluble fractions of Pb. For example, assuming that 15% of water-soluble components for total Pb were contained in fine mode, Pb concentrations for our samples would be expected to increase by roughly 30 $ng \cdot m^{-3}$ in fine mode, which can present a bimodal size distribution with the peaks in fine and coarse modes; however, the coarse mode still surpasses the fine mode in terms of mass concentration.

The elemental mass concentrations determined using PIXE were used to calculate the enrichment factor (EF) of the coarse and fine particles collected in Japan. We segregated the particles collected by the low-pressure impactor into two types: fine and coarse particles with aerodynamic diameters of less than and greater than 1.2 μm respectively. The separation size of 1.2 μm corresponds to the 50% cut-off aerodynamic diameter of stage P5 for the impactor.

EF, which is widely employed in the identification of anthropogenic sources for metallic elements, is defined as follows:

$$EF_X = [X/Y]_{air} / [X/Y]_{crust} \quad (4)$$

where EF_X is the EF of species X; Y, a reference element for the crustal material; $[X/Y]_{air}$ is the ratio of the amount of species X to that of species Y in the aerosol sample; and $[X/Y]_{crust}$ is the ratio of the amount of species X to that of species Y in the crust. Aluminum was selected as the reference element and the value of $[X/Al]_{crust}$ was obtained from a previous study (Taylor, 1964). The EF of Ca was determined from the total concentration of water-insoluble and ionic components. Concentrations of water-insoluble components were used to determine the EF of other elements. The EF values of Si, Ca, Ti, Mn, and Fe approached unity; this indicates that the source of these elements was the crust, as shown in Fig. 10. The high EF of Cr, Ni, Cu, Zn, and Pb in the fine mode indicates that these elements were derived from a different pollutant source. The EF of Pb (273) is considerably higher than that of other elements and the EF of Pb in the coarse mode is also high (40). It is assumed that *Kosa* dust mixed with

anthropogenic Pb pollutants along its transport path is the source of Pb in the coarse mode fraction.

3.2.2. Ionic components

Figure 11 shows the size distributions for the equivalence concentrations of the major ions. The size distributions of Cl^-, NO_3^-, Na^+, NH_4^+, and Ca^{2+} were unimodal while those of SO_4^{2-} were bimodal. NH_4^+ was the major ion in the fine mode fraction while Ca^{2+}, Cl^-, and NO_3^- were present in abundance in the coarse mode fraction. Since most of the Ca^{2+} is derived from soil, it is predominantly present in the coarse mode fraction. The observation site at Yasaka is located ~6 km from the sea at the center of the Tango peninsula; therefore, the presence of Na^+ and Cl^- in the coarse mode fraction is attributed to sea salt. The equivalence ratio of Cl^- to Na^+ in the aerosols is lower than that in seawater, suggesting chlorine loss from sea salt aerosols.

3.2.3. XAFS analysis

Figure 12 shows the Pb L3 edge XANES spectra of various reference materials, including the two samples collected using the high-volume samplers at Yasaka and Byunsan. The spectra of the *Kosa* samples collected from these two locations exhibit remarkably similar shapes. A comparison of the spectra of the *Kosa* samples with the reference materials indicated that Pb in the samples consists of several compounds instead of being a single species. Since the actual chemical species of the samples are unknown, we needed to select major reference Pb materials in order to regenerate the original XANES spectra of the samples using LCF.

Initially, Pb compounds that originate from soil were excluded owing to their high EF_{Pb} values. Previous studies (Mori et al., 2003; Sun et al., 2005; Hioki et al. 2006) have reported that Pb in *Kosa* aerosols is mostly derived from anthropogenic sources, which is a reasonable premise. PbO and $PbSO_4$ were chosen as candidate materials because they are the major constituents of anthropogenic Pb aerosols (Sobanska et al., 1999; Gieré et al., 2006; Jiang et al., 2007, Funasaka et al., 2008). $PbCl_2$ was

also chosen since it is a typical water-soluble component. Furthermore, $PbCO_3$ was selected on account of the conversion of $PbSO_4$ into $PbCO_3$ during the transport. Finally, spectral fits performed for PbO, $PbSO_4$, $PbCl_2$, and $PbCO_3$ yielded a satisfactory residual value *R*; *R* did not improve when spectral fits with other combinations of reference materials such as PbO, $PbSO_4$, and $PbCO_3$ was performed.

Table 6 indicates the molar percentages of the reference materials chosen above relative to the total Pb obtained by LCF. PbO, $PbSO_4$, $PbCl_2$, and $PbCO_3$, respectively, account for 52%, 27%, 15%, and 5% of the total Pb in the sample obtained from Korea; Pb existed primarily as PbO and $PbSO_4$. This result suggests that the partial transformation of $PbSO_4$ to $PbCO_3$ had already occurred before the arrival of *Kosa* particles at Byunsan or primary $PbCO_3$ particles were transported. Under the assumption that the presence of $PbCO_3$ in the *Kosa* samples was entirely due to the conversion of $PbSO_4$ into $PbCO_3$, the molar percentage of $PbCO_3$ relative to the total amount of $PbCO_3$ and $PbSO_4$ is ~18%. This value is significantly larger than the value obtained in the laboratory experiments (4%) under conditions of exposure to high humidity (Run 2) and contact with small amount of NaCl particles (Run 3). If the $PbSO_4$ and *Kosa* particles underwent a cloud process from the continent to Korea—i.e. immersion in water—the $PbCO_3$ fraction in the total Pb content for all the samples would be higher than what was measured. Another possibility is the occurrence of internal mixing of the mineral particles with hygroscopic particles such as sea salt and $(NH_4)_2SO_4$. The deliquescence of these mixtures led to the formation of a thin water film around the *Kosa* particles under conditions of high humidity during their transport; this water film may provide the reaction site for $PbCO_3$ formation from $CaCO_3$ and $PbSO_4$.

The percentages of PbO, $PbSO_4$, $PbCl_2$, and $PbCO_3$ relative to the total Pb content were 44%, 30%, 21%, and 5%, respectively, for the sample obtained in Japan. The fraction of water-soluble $PbCl_2$ is comparable to that reported by Funasaka et al. (2008). XANES analysis demonstrated that no significant difference was found in the chemical forms of Pb between the two samples collected at Bynsan and Yasaka. On the basis of the NOAA HYSPLIT4 back-trajectory analysis, the air mass was transported in a marine boundary layer without anthropogenic lead sources after Korea. Therefore, we postulate that

definite transformation did not occur during the transport of *Kosa* particles from Korea to Japan.

4. Conclusions

Laboratory experiments using test particles of $CaCO_3$ and $PbSO_4$ revealed the formation of stick or needle particles following the immersion of both particles in a water droplet, in addition to the existence of NaCl particles attached to the test particles under conditions of higher RH than DRH. The morphological change in the particles was quantitatively evaluated using their aspect ratios. The distributions of the aspect ratios indicated a shift to a right tail distribution with a peak of 2.8 in the case of samples immersed in a water droplet and a peak at 1.6 in the case of unreacted samples. Several quantities of stick crystals were formed through the transformation of particles in the presence of water. A minute peak in large value appeared for the samples on which NaCl particles were attached in an atmosphere with RH greater than 80%, while the samples without attached NaCl particles did not exhibit this distribution change even after being held in the same atmospheric conditions. Spectral analysis of the XANES spectroscopy measurements of the samples immersed in the water droplet revealed that 60–80% of $PbSO_4$ particles converted to $PbCO_3$ after 24 h, contrary to the ~4% conversion observed for samples not immersed in the water droplet.

XANES spectroscopy was applied to field samplings of the aerosols during a *Kosa* event in Japan and Korea in order to determine the chemical forms of Pb in the *Kosa* particles. The shapes of the XANES spectra of both these samples were almost similar. The molar percentages of PbO, $PbSO_4$, $PbCl_2$, and $PbCO_3$ were approximately 44%, 30%, 21%, and 5%, respectively, in samples collected in Japan; no significant differences were observed in the samples collected over Korea. Therefore, definite transformation did not occur during the transport of *Kosa* particles from Korea to Japan. XANES analysis was performed for bulk samples due to analytical reasons. Analysis of the size-segregated samples will be required to clearly determine the transformation process in the future. Furthermore, the

speciation of chemical forms for Pb particles of the continent is also required.

Acknowledgements

This research was partially supported by funds from the Grant-in-Aid for Scientific Research (B) under Grant No. 19310021 and from the Grant-in-Aid for Scientific Research on Innovative Areas under Grant No. 2012005 from the Japanese Ministry of Education, Culture, Sports, Science and Technology (MEXT). The authors express their sincere gratitude to Prof. G.-U. Kang for his sampling at Byunsan. Synchrotron radiation experiments were performed at SPring-8 with approval from the Japan Synchrotron Radiation Research Institute (JASRI) (Proposal No. 2007B1962). The authors gratefully acknowledge the NOAA Air Resources Laboratory (ARL) for the provision of the HYSPLIT back trajectory model used in the present study.

References

Barltrop, D. and Meek, F., 1975. Absorption of different lead compounds. Postgraduate Medical Journal 51, 805-809.

Bates, T.S., Quinn, P.K., Coffman, D.J., Covert, D.S., Miller, T.L., Johnson, J.E., Carmichael, G.R., Uno, I., Guzaaotti, S.A., Sodeman, D.A., Prather, K.A., Rivera, M., Russell, L.M. and Merrill, J.T., 2004. Marine boundary layer dust and pollutant transport associated with the passage of a frontal system over estern Asia. Journal of Geophysical Research 109, 2D19S19, doi:10.1029/2003JD004094.

El-Korashy, S.A., 2003. Studies on divalent ion uptake of transition metal cations by calcite through crystallization and cation exchange process. Journal of Materials Science 38, 1709-1719.

Erel, Y., Dayan, U., Rabi, R., Rudich, Y. and Stein, M., 2006. Trans boundary transport of pollutants by atmospheric mineral dust. Environmental Science and Technology 40, 2996-3005.

Falgayrac, G., Sobanska, S., Laureyns, J. and Brèmard, C., 2006. Heterogeneous chemistry between $PbSO_4$ and calcite microparticles using Raman microimaging. Spectrochimica Acta A 64,

1095-1101.

Funasaka, K., Tojo, T., Katahira, K.., Shinya, M., Miyazaki, T., Kamiura, T., Yamamoto,O., Moriwaki, H., Tanida, H. and Takaoka, M., 2008. Detection of Pb-LIII edge XANES spectra of urban atmospheric particles combined with simple acid extraction. Science of the Total Environment 403, 230-234.

Gieré, R., Blackford, M. and Smith, K., 2006. TEM study of $PM_{2.5}$ emitted from coal and tire combustion in a thermal power station. Environmental Science and Technology 40, 6235- 6240.

Godelitsas, A., Astilleros, J.M., Hallam, K., Harissopoulos, S. and Putnis, A., 2003. Interaction of calcium carbonates with lead in aqueous solutions. Environmental Science and Technology 37, 3351-3360.

Goodman, A.L., Underwood, G.M. and Grassian, V.H., 2000. A laboratory study of heterogeneous reaction of nitric acid on calcium carbonate particles. Journal of Geophysical Research 105, 29053-29064.

Han, J.S., Moon, K.J., Ahn, J.Y., Hong, Y.D., Kim, Y.J., Ryu, S.Y., Cliff, S.S. and Cahill, T.A., 2004. Characteristics of ion components and trace elements of fine particles at Gosan, Korea in spring time from 2001 to 2002. Environmental Monitoring and Assessment 92, 73-93.

Hand, J.L., Mahowald, N.M., Chen, Y., Siefert, R.L., Luo, C., Subramaniam, A. and Fung, I., 2004. Estimates of atmospheric-processed soluble iron from observations and a global mineral aerosol model: Biogeochemical implications. Journal of Geophysical Research 109, D17205, doi:10.1029/2004JD004574.

Hioki, T., Nakanishi, S., Mukai, H. and Murano, K., 2006. Analysis of long-range transport of aerosols with water-soluble ionic species and trace metal components, collected continuously with particle size segregation in the coastal area of the sea of Japan –Focusing on the Kosa event in spring 2002. Earozoru Kenkyu (Journal of Aerosol Research) 21, 160 – 175 (in Japanese).

International Energy Agency (IEA), 2007. World Energy Outlook 2007, China and India Insights.

Jiang, J.-G., Xu, X., Wang, J. and Yang, S.-J., and Zhang, Y., 2007. Investigation of basic properties of fly ash from urban waste incinerators in China. Journal of Environmental Science 19, 458–463.

Karanasiou, A.A., Sitaras, I.E., Siskos, P.A. and Eleftheriadis, K., 2007. Size distribution and sources of trace metals and n-alkanes in the Athens urban aerosol during summer. Atmospheric Environment 41, 2368-2381.

Krueger, B.J., Grassian, V.H., Laskin, A. and Cowin, J.P., 2003. The transformation of solid atmospheric particles into liquid droplets through heterogeneous chemistry: Laboratory insights into the processing of calcium containing mineral dust aerosol in the troposphere. Geophysical Research Letters 30, 1148, doi:10.1029/2002GL016563.

Krueger, B.J., Grassian, V.H., Cowin, J.P.and Laskin, A., 2004. Heterogeneous chemistry of individual mineral dust particles from different dust source regions: the importance of particle mineralogy. Atmospheric Environment 38, 6253-6261.

Lee, C.S.L., Li, X.-D., Zhang, G., Li, J., Ding, A.-J. and Wang, T., 2007. Heavy metals and Pb isotopic composition of aerosols in urban and suburban areas of Hong Kong and Guzngzhou, South China-Evidence of the long-range transport of air contaminants. Atmospheric Environment 41, 432-447.

Ma, C.-J., Tohno, S., Kasahara, M. and Hayakawa, S., 2004a. Properties of individual Asian dust storm particles collected at Kosan, Korea during ACE-Asia. Atmospheric Environment 38, 1133-1143.

Ma, C.-J., Tohno, S., Kasahara, M. and Hayakawa, S., 2004b. The nature of individual solid particles retained in size-resolved raindrops fallen in Asian dust storm event during ACE-Asia. Atmospheric Environment 38, 2951-2964.

Marx, S.K., Kamber, B.S. and McGowan, H.A., 2008. Scavenging of atmospheric trace metal pollutants by mineral dusts: Inter-regional transport of Australian trace metal pollution to New Zealand. Atmospheric Environment 42, 2460-2478.

Matsumoto, K., Uyama, Y., Hayano, T., and Uematsu, M., 2004. Transport and chemical transformation

of anthropogenic and mineral aerosol in marine boundary layer over the western North Pacific. Journal of Geophysical Research 109, D21206, doi:10.1029/2004JD004696.

Maxwell, J.A., Teesdate, W.J. and Campbell, J.L., 1995. The Guelp PIXE software package II. Nuclear Instruments and Methods in Physics Research B95, 407-421.

Mori, I., Nishikawa M., Tanimura, T. and Quan, H., 2003. Change in size distribution and chemicalcomposition of kosa (Asian dust) aerosol during long-range transport. Atmospheric Environment 37, 4253-4263.

Morikawa, A., Tohno, S. and Kasahara, M., 2006 Analysis of short-time variation of modified components in Asian dust particles by single particle analysis. Earozoru Kenkyu (Journal of Aerosol Research) 21, 239-246 (in Japanese).

Morikawa, A., Ishizaka, T. and Tohno, S., 2007. Heterogeneous reactivity of sulfate coated $CaCO_3$ particles with gaseous nitric acid, in: O'Dowd, C. and Wagner, P.E. (Eds.), Nucleation and Atmospheric Aerosols: 17th International Conference, Galway, Ireland, 2007, Springer Verlag, pp.994-998.

Nishikawa, M., Kanamori, S., Kanamori, N. and Mizoguchi, T., 1991. Kosa aerosol as eolian carrier of anthropogenic material. Science of the Total Environment 107, 13-27.

Okuda, T., Kato, J., Mori, J., Tenmoku, M., Suda, Y., Tanaka, S., He, K., Ma, Y., Yang, F., Yu, X., Duan, F. and Lei, Y., 2004.: Daily concentrations of trace metals in aerosols in Beijing, China, determined by using inductively coupled plasma mass spectrometry equipped with laser ablation analysis, and source identification of aerosols. Science of the Total Environment 330, 145 - 158.

Pakkanen, T.A., Kerminen, V.-M., Loukkola, K., Hillamo, R.E., Aarnio, P., Koskentalo, T. and Maenhaut, W., 2003. Size distributions of mass and chemical components in street-level and rooftop PM1 particles in Helsinki. Atmospheric Environment 37, 1673-1690.

Roberts, D., Scheinost, A.C. and Sparks, D.L., 2003. Zinc speciation in contaminated soils combining direct and indirect characterization methods, in: Selim, H.M. and Kingery, W.L. (Eds.), Geochemical

and Hydrological Reactivity of Heavy Metals in Soils, Lewis Publishers: Boca Raton, FL, pp.188-227.

Sarks, D.L., 2005. Metal and oxyanion sorption on naturally occurring oxide and clay mineral surfaces, in: Grassian, V.H. (Ed.), Environmental Catalysis, Taylor & Francis, pp.3 - 36.

Singh, M., Jaques, P.A. and Sioutas, C., 2003. Size distribution and diurnal characteristics of particle-bound metals in source and receptor sites of the Los Angeles Basin. Atmospheric Environment 36, 1675-1689.

Sobanska, S., Ricq, N., Laboudigue, A., Guillermo, R., Brémard, C., Laureyns, J., Merlin, J.C. and Wignavourt, J.P., 1999. Microchemical investigations of dust emitted by a lead smelter. Environmental Science and Technology 33, 1334-1339.

Sun, Y., Zhuang, G., Wang, Y., Zhao, X., Li, J., Wang, Z. and An Z., 2005. Chemical composition of dust storms in Beijing and implications for the mixing of mineral aerosols with pollution aerosol on the pathway. Journal of Geophysical Research 110, D24209, doi:10.1029/2005JD006054.

Sun, Y., Zhuang, G., Zhang, W., Wang, Y. and Zhuang, Y., 2006 Characteristics and sources of lead pollution after phasing out leaded gasoline in Beijing. Atmospheric Environment 40, 2973-2985.

Taguchi, T., Ozawa, T. and Yashiro, H.: REX2000, 2005. Yet another XAFS analysis package. Physica Scripta T115, 205–206.

Takaoka, M., Shiono, A., Nishimura, K., Yamamoto, T., Uruga, T., Takeda, N., Tanaka, T., Oshita, K., Matsumoto, T. and Harada, H., 2005. Dynamic change of copper in fly ash during de Novo synthesis of dioxins. Environmental Science and Technology 39, 5878-5884.

Taylor, S.R., 1964. Abundance of chemical elements in the continental crust: a new table. Geochimica Cosmochimca Acta 28, 1273-1285.

Tohno, S., Ma, C.-J., Hayakawa, S., Yamasaki, S. and Kasahara, M., 2006. Single particle analysis for chemical characterization of atmospheric aerosols: Application of X-ray microprobe system and double thin film method. Environmental Monitoring and Assessment 120, 575-584.

Trochkine, D., Iwasaka, Y., Matsuki, A., Yamada, M., Kim, Y.-S., Zhang, D., Shi, G.-Y., Shen , Z. and Li, G., 2003. Comparison of the chemical composition of mineral particles collected in Dunhuang, China and those collected in the free troposphere over Japan: Possible chemical modification during long-range transport. Water, Air and Soil Pollution Focus 3, 161–172.

Zhang, D. and Iwasaka, Y., 1999. Nitrate and sulfate in individual Asian dust-storm particles in Beijing, China in spring of 1995 and 1996. Atmospheric Environment 33, 3213-3223.

Zhang, D. and Iwasaka, Y., 2004. Size change of Asian dust particles caused by sea salt interaction: Measurement in southwestern Japan. Geophysical Research Letters 31, L15102, doi:10.1029/2004GL020087.

Legends

Table 1 Samples used for XANES measurements and the corresponding reaction times

Table 2 Molar percentages of $PbSO_4$ and $PbCO_3$ relative to the total Pb content after reaction

Table 3 Molar percentages of various chemical forms relative to the total Pb content in the particles collected during the *Kosa* event

Fig. 1. Temporal variation of the size-segregated concentration of aerosols, ground temperature, and RH at Yasaka during the sampling period.

Fig. 2. Map showing sampling sites and the NOAA HISPILIT backward trajectories for the air parcels that arrived in Yasaka at 20 UTC 31 Mar 2007.

Fig. 3. Mass size distributions of $CaCO_3$ and $PbSO_4$ particles used in laboratory experiments.

Fig. 4. SEM pictures of sample particles. (a) $PbSO_4$ particles before reaction, (b) $CaCO_3$ particles before reaction, and (c) morphology of $CaCO_3$ and $PbSO_4$ particles after immersion in a water droplet for 3 h and subsequent drying. Peaks of Al and Cu originated from the sample stage for SEM observation.

Fig. 5. Morphology of NaCl-adsorbed $CaCO_3$/$PbSO_4$ particles after being exposed to humid air for 3 h and subsequent drying. Peaks of Al and Cu originated from the sample stage for SEM observation.

Fig. 6. Distributions of the aspect ratios for $CaCO_3$/$PbSO_4$ particles under the following three experimental conditions: 1) Immersion in a water droplet, 2) adsorption of NaCl particles in an atmosphere with a RH of 95%, and 3) exposure to an atmosphere with a RH of 95%. The aspect ratios were determined for 211 particles in sample 1) and 200 particles in samples 2) and 3).

Fig. 7. Pb L3 edge XANES spectra of the samples and the reference materials $PbSO_4$ and $PbCO_3$

Fig. 8. Total mass size distributions of aerosols sampled during the *Kosa* event at Yasaka (top) and Byunsan (bottom).

Fig. 9. Total mass size distributions of Si and Pb in the water-insoluble components of the aerosols sampled during the *Kosa* event at Yasaka.

Fig. 10. Enrichment factors of metal constituents in coarse and fine particles collected during the *Kosa* event at Yasaka.

Fig. 11. Size distributions of the equivalence concentrations of major ions in the aerosols sampled at Yasaka during the *Kosa* event

Fig. 12. Pb L3 edge XANES spectra of the various reference materials and the two samples collected using high-volume samplers during the *Kosa* event at Yasaka and Byunsan.

1

Table 1

Samples used for XANES measurements and the corresponding reaction times

Mass of the compounds (mg)	Immersion in water		Humid atmosphere		Humid atmosphere with NaCl particles		Bulk sample in water
	A1	A2	B1	B2	C1	C2	D
$PbSO_4$	0.51	0.53	0.65	0.18	1.32	0.25	8.68
$CaCO_3$	30	1.2	1.4	1.4	3.5	1.4	52.2
NaCl	-	-	-	-	0.020	0.020	-
RH (%)	-		95		95		-
Reaction time (day)	1		1		1		3

Table 2

Molar percentages of $PbSO_4$ and $PbCO_3$ relative to the total Pb content after reaction

Sample	A1	A2	B1	B2	C1	C2	D
$PbSO_4$ (%)	39.0	12.4	97.0	96.4	96.0	96.1	7.9
$PbCO_3$ (%)	61.0	87.6	3.0	3.6	4.0	3.9	92.1
R	0.013	0.010	0.013	0.012	0.011	0.011	0.013

R: residual value

Table 3

Molar percentages of various chemical forms relative to the total Pb content in the particles collected during the *Kosa* event

Site	PbO (%)	$PbSO_4$ (%)	$PbCO_3$ (%)	$PbCl_2$ (%)	R
Byunsan, Korea	52.1	27.4	5.1	15.4	0.010
Yasaka, Japan	44.0	30.1	4.7	21.1	0.008

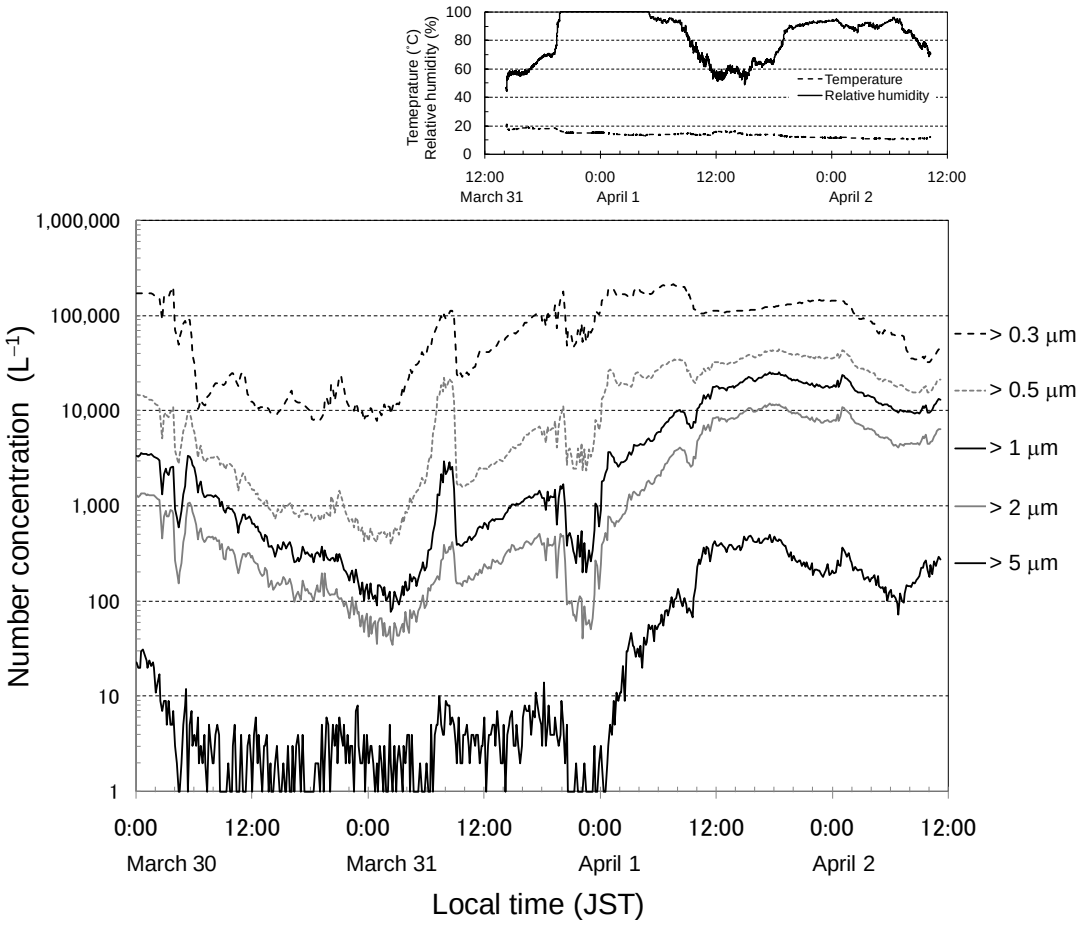

Fig. 1. Temporal variation of the size-segregated concentration of aerosols, ground temperature, and RH at Yasaka during the sampling period.

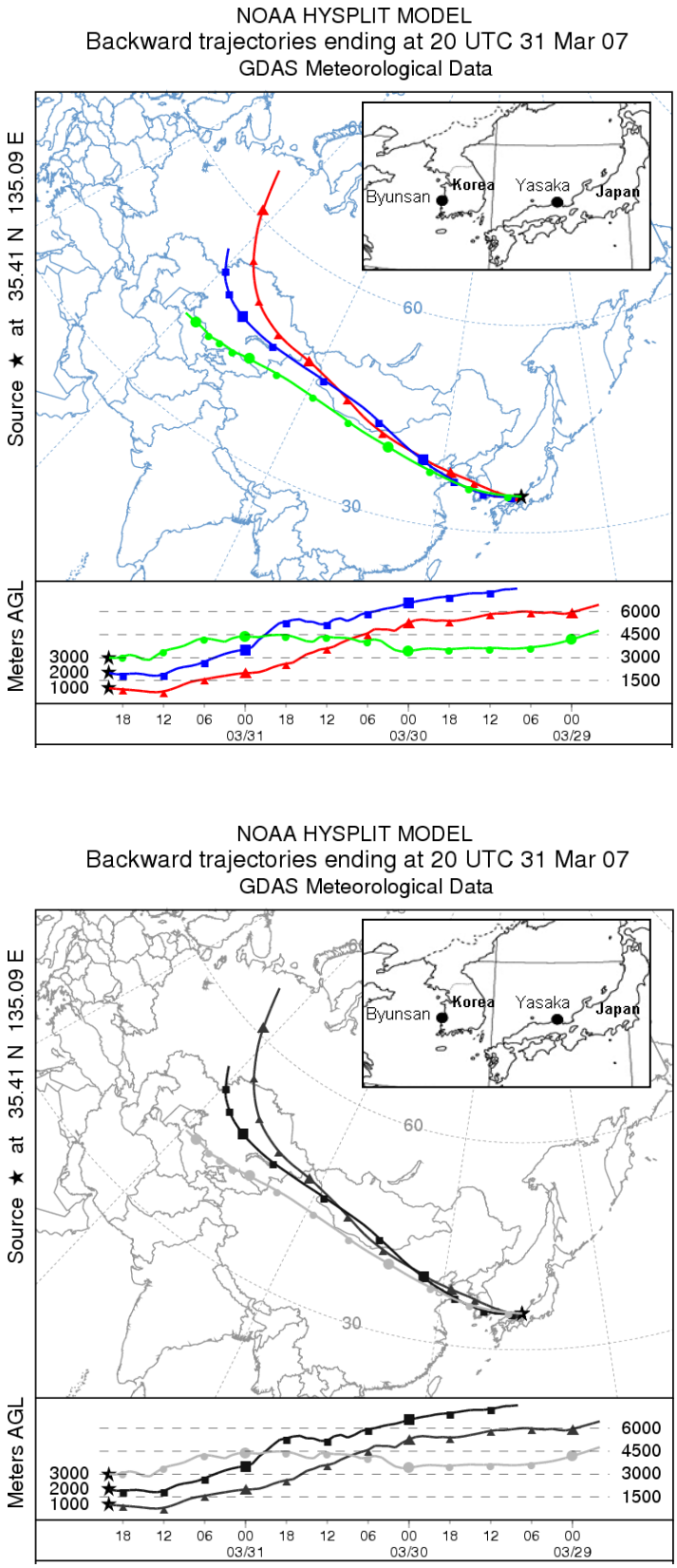

Fig. 2. Map showing sampling sites and the NOAA HISPILIT backward trajectories for the air parcels that arrived in Yasaka at 20 UTC 31 Mar 2007.

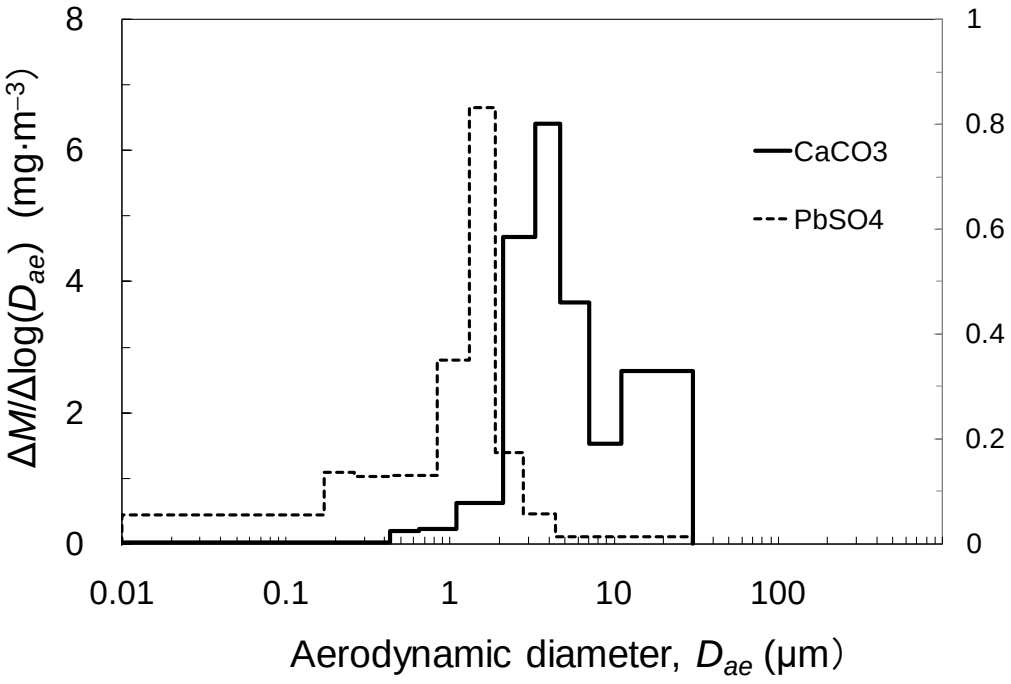

Fig. 3. Mass size distributions of $CaCO_3$ and $PbSO_4$ particles used in laboratory experiments.

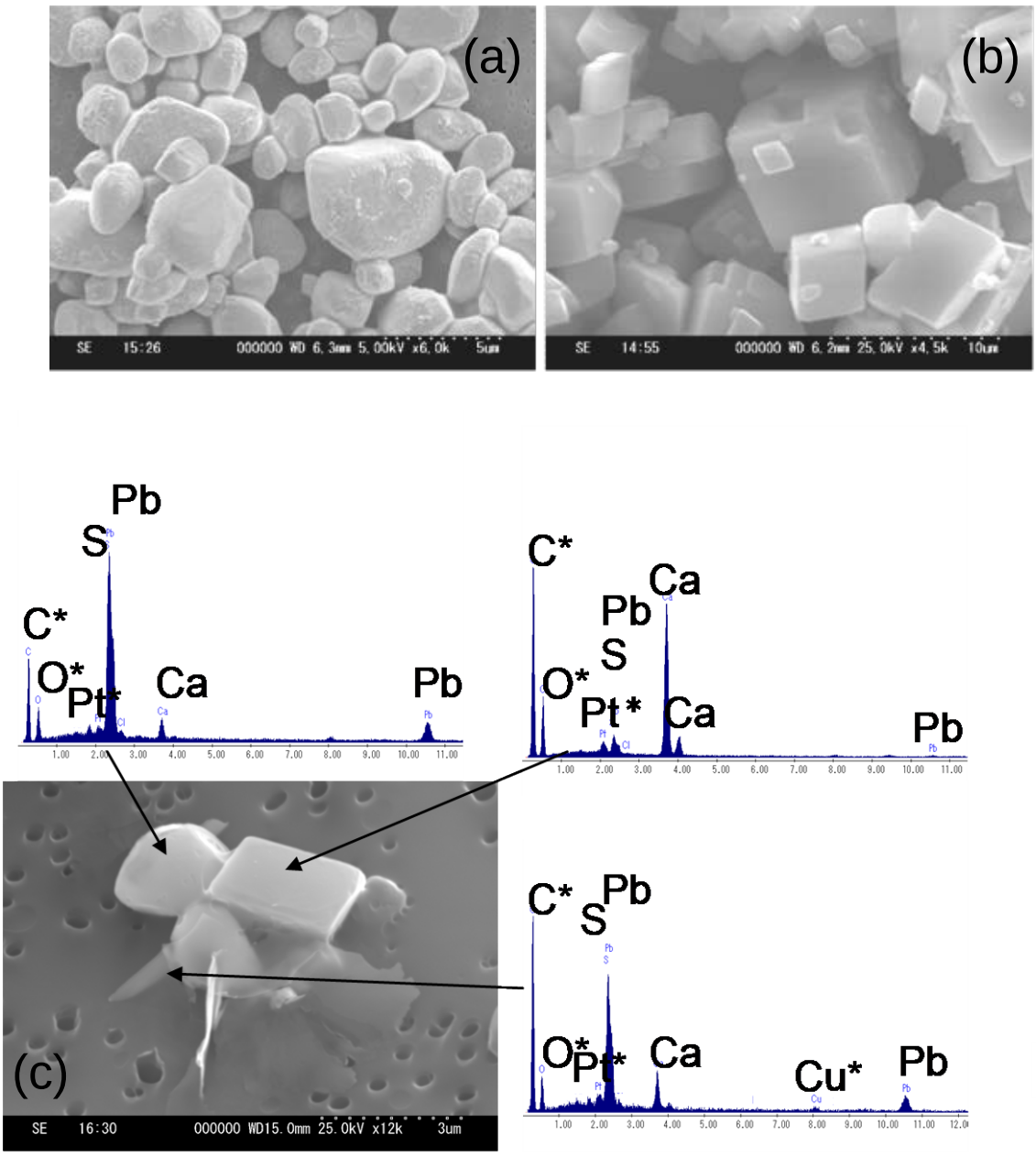

Fig. 4. SEM pictures of sample particles. (a) $PbSO_4$ particles before reaction, (b) $CaCO_3$ particles before reaction, and (c) morphology of $CaCO_3$ and $PbSO_4$ particles after immersion in a water droplet for 3 h and subsequent drying. Peaks of Al and Cu originated from the sample stage for SEM observation.

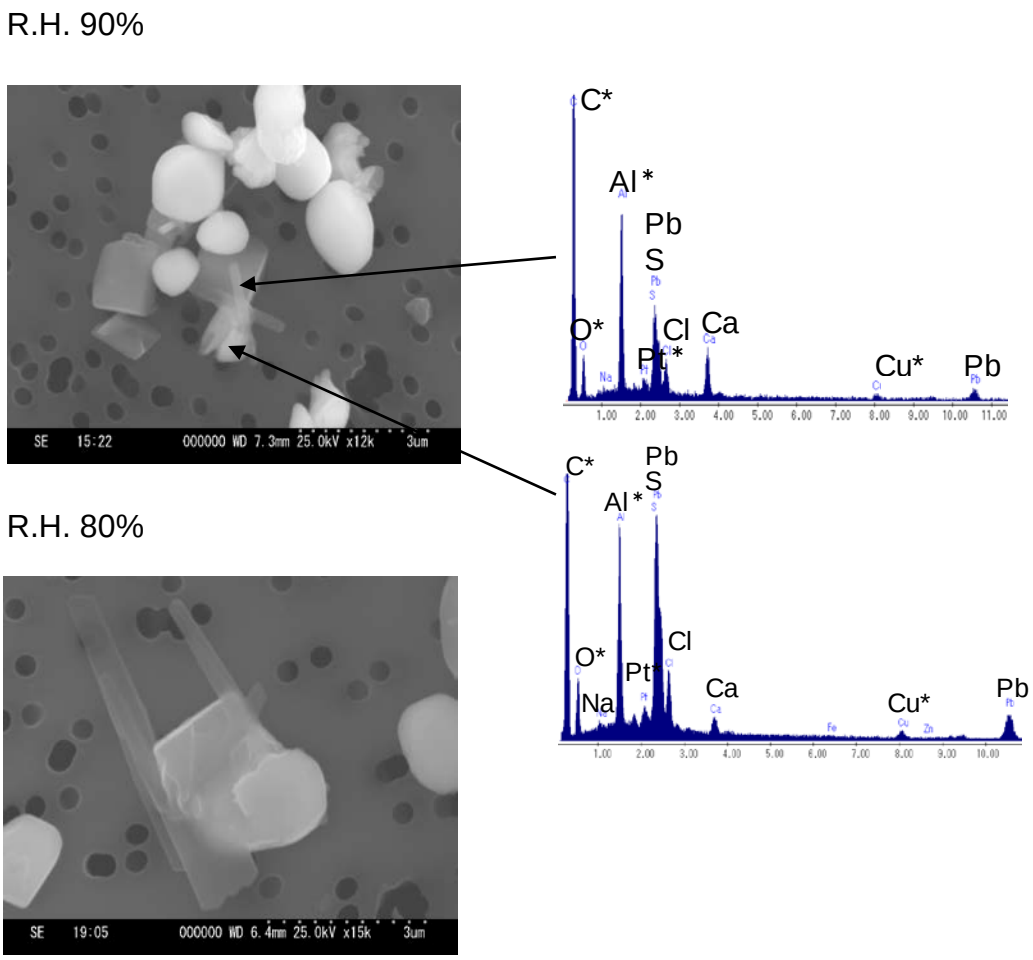

Fig. 5. Morphology of NaCl-adsorbed $CaCO_3$/$PbSO_4$ particles after being exposed to humid air for 3 h and subsequent drying. Peaks of Al and Cu originated from the sample stage for SEM observation.

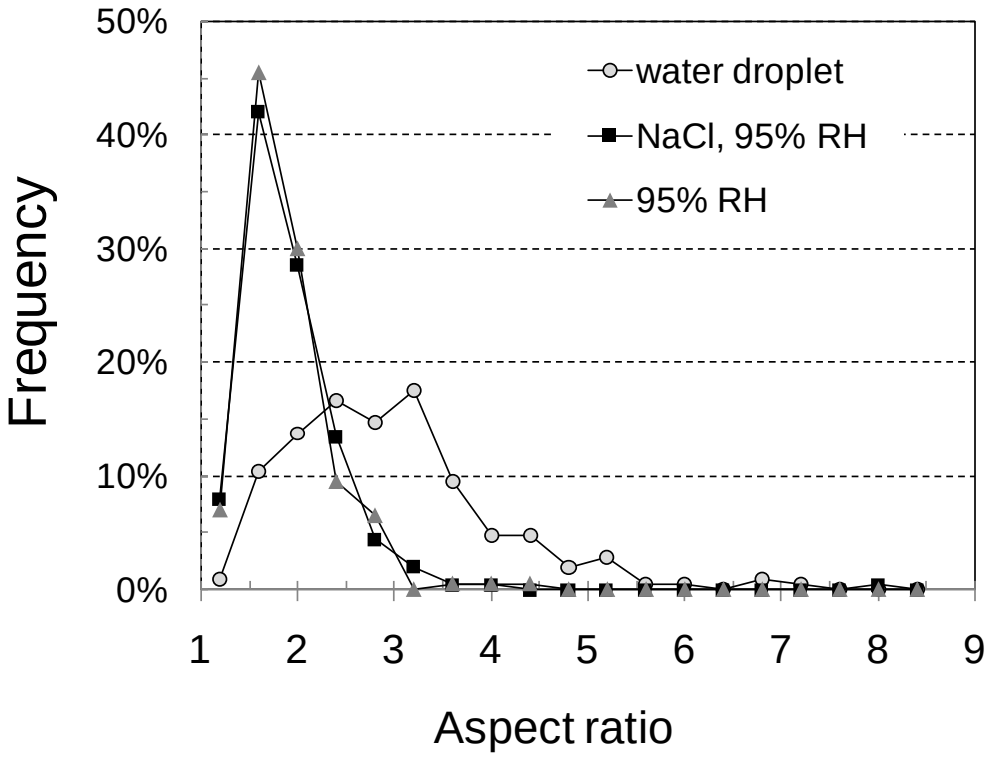

Fig. 6. Distributions of the aspect ratios for $CaCO_3$/$PbSO_4$ particles under the following three experimental conditions: 1) Immersion in a water droplet, 2) adsorption of NaCl particles in an atmosphere with a RH of 95%, and 3) exposure to an atmosphere with a RH of 95%. The aspect ratios were determined for 211 particles in sample 1) and 200 particles in samples 2) and 3).

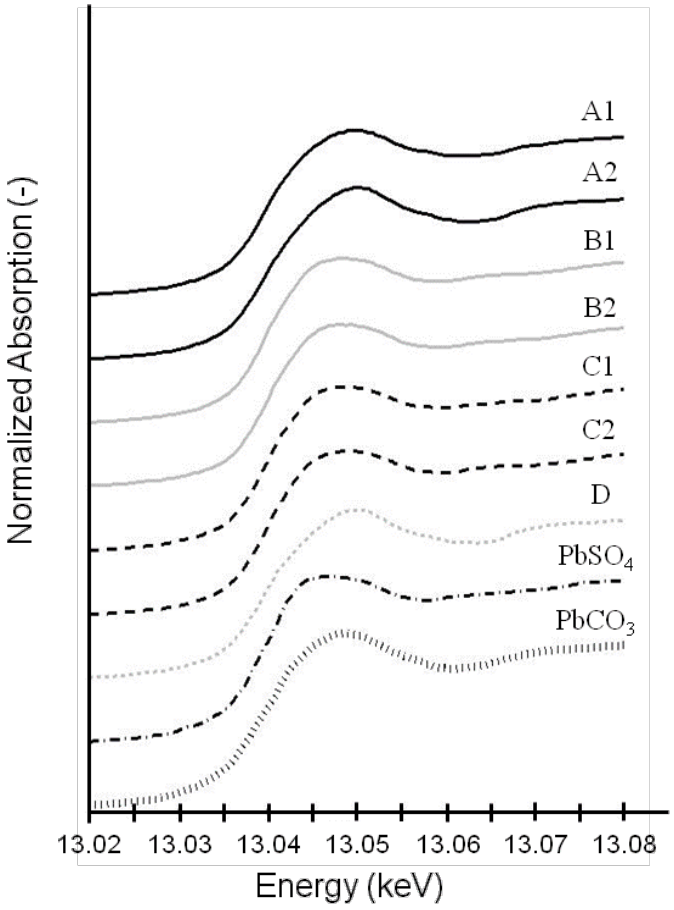

Fig. 7. Pb L3 edge XANES spectra of the samples and the reference materials $PbSO_4$ and $PbCO_3$.

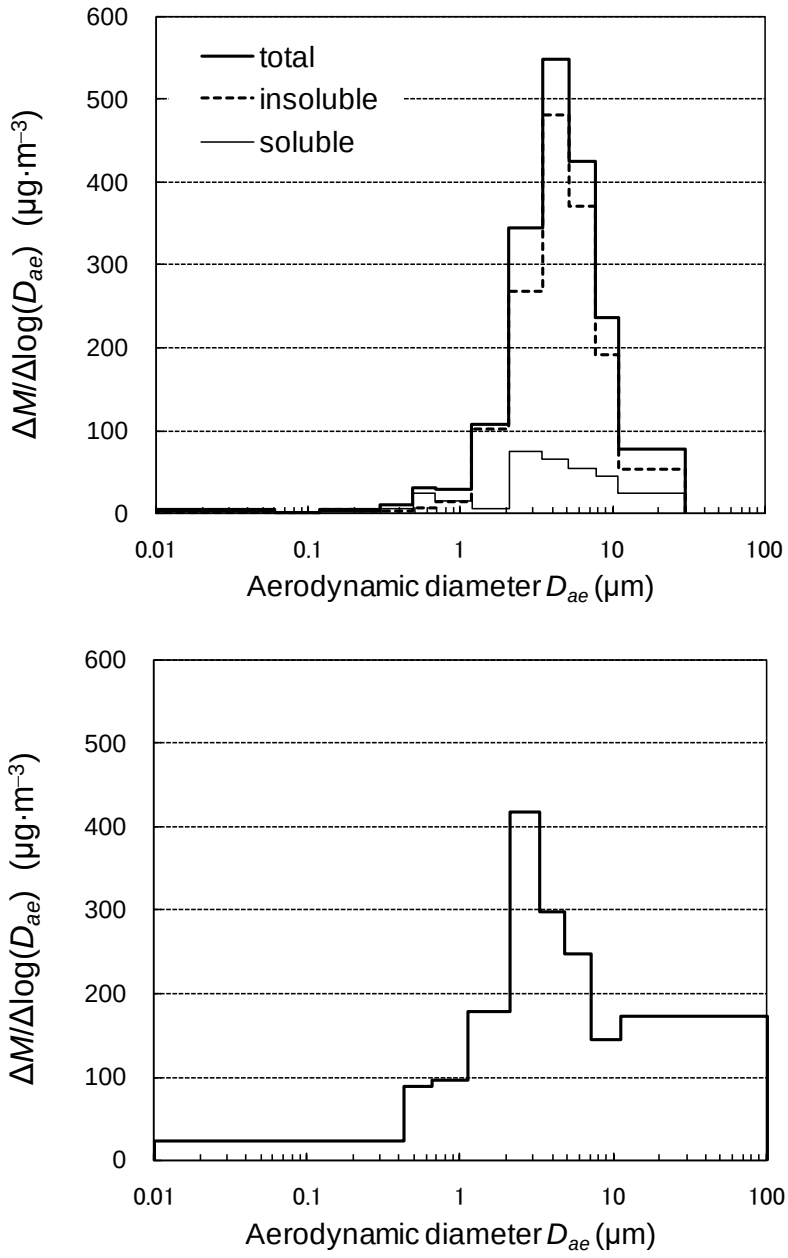

Fig. 8. Total mass size distributions of aerosols sampled during the *Kosa* event at Yasaka (top) and Byunsan (bottom).

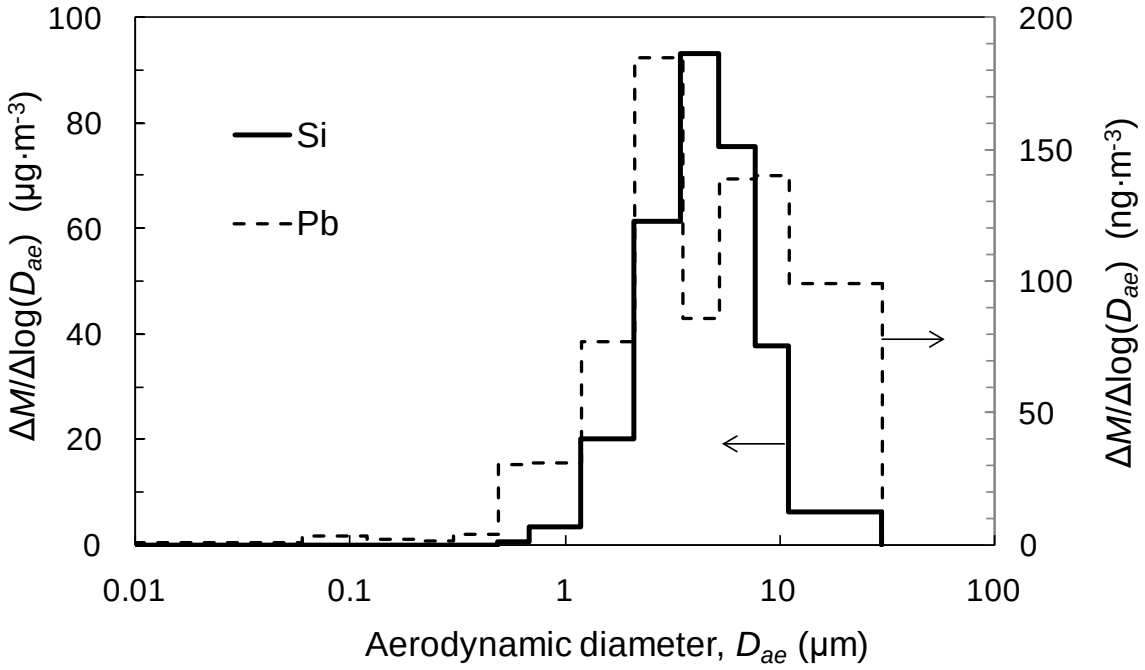

Fig. 9. Mass size distributions of Si and Pb in the water-insoluble components of the aerosols sampled during the *Kosa* event at Yasaka.

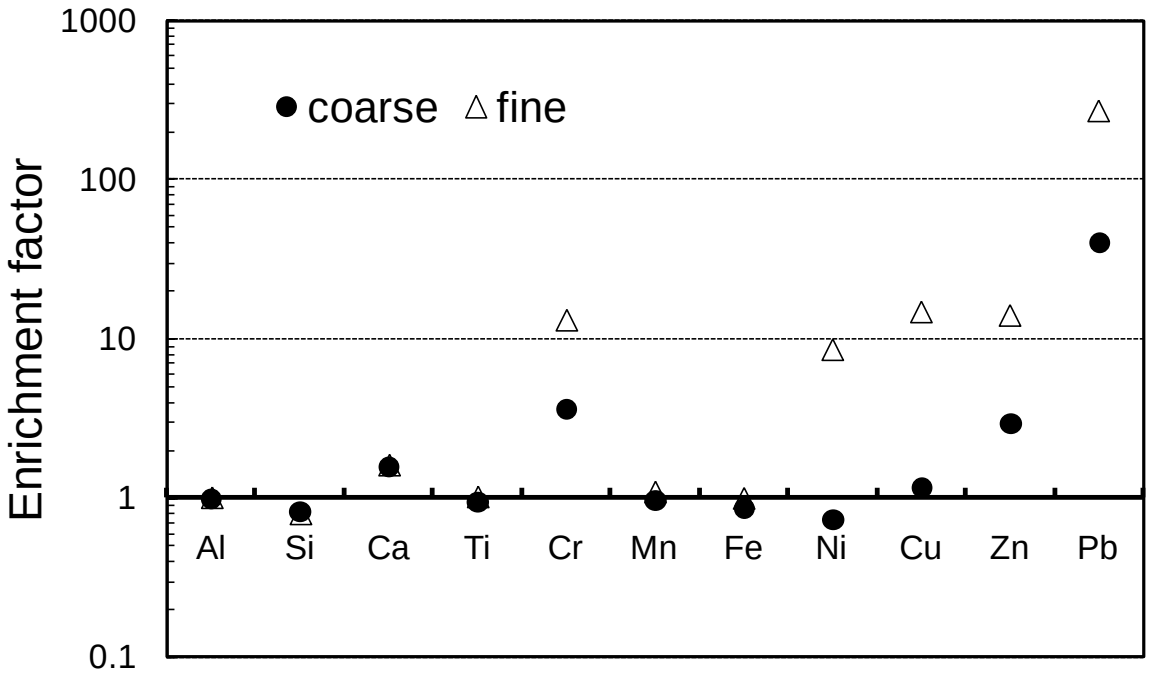

Fig. 10. Enrichment factors of metal constituents in coarse and fine particles collected during the *Kosa* event at Yasaka.

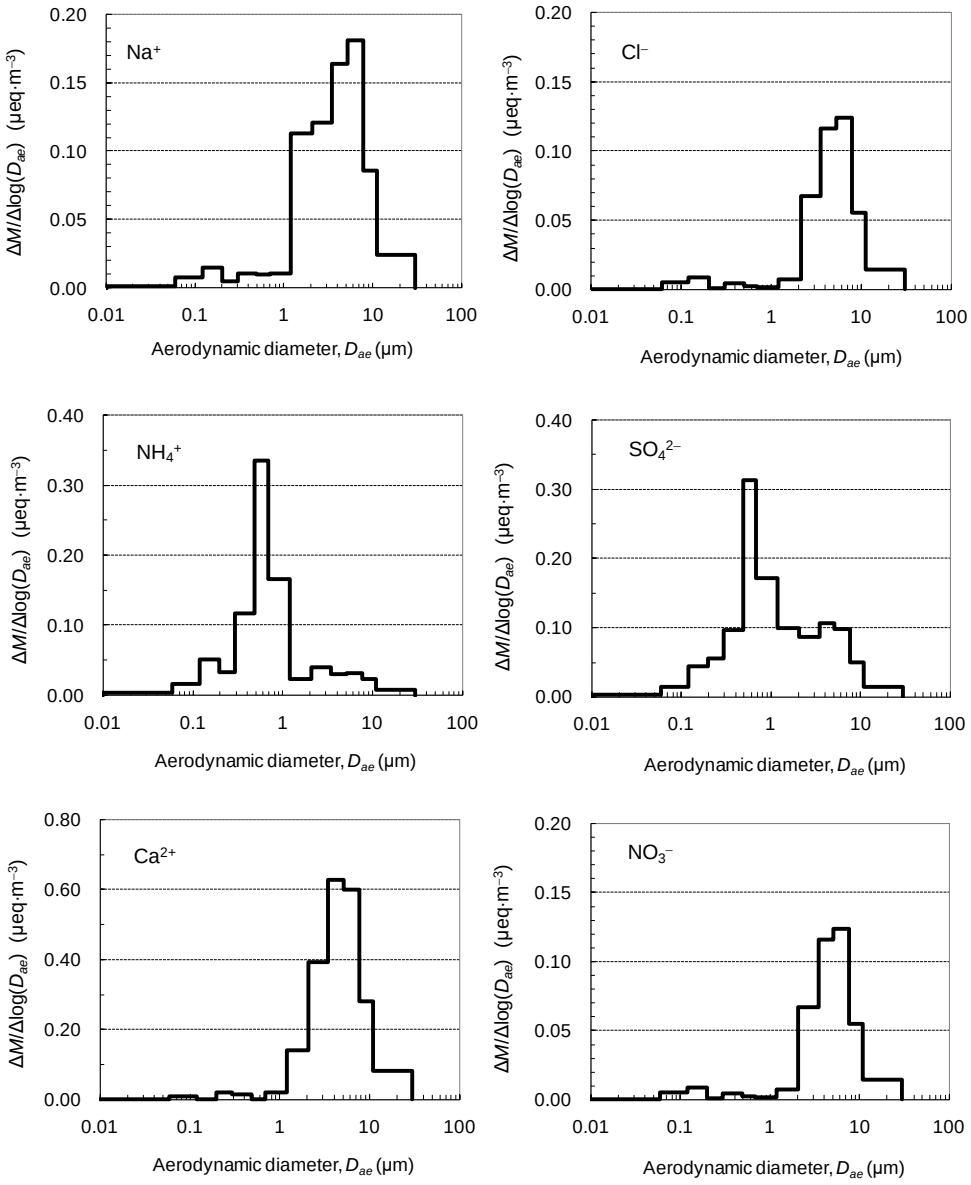

Fig. 11. Size distributions of the equivalence concentrations of major ions in the aerosols sampled at Yasaka during the *Kosa* event.

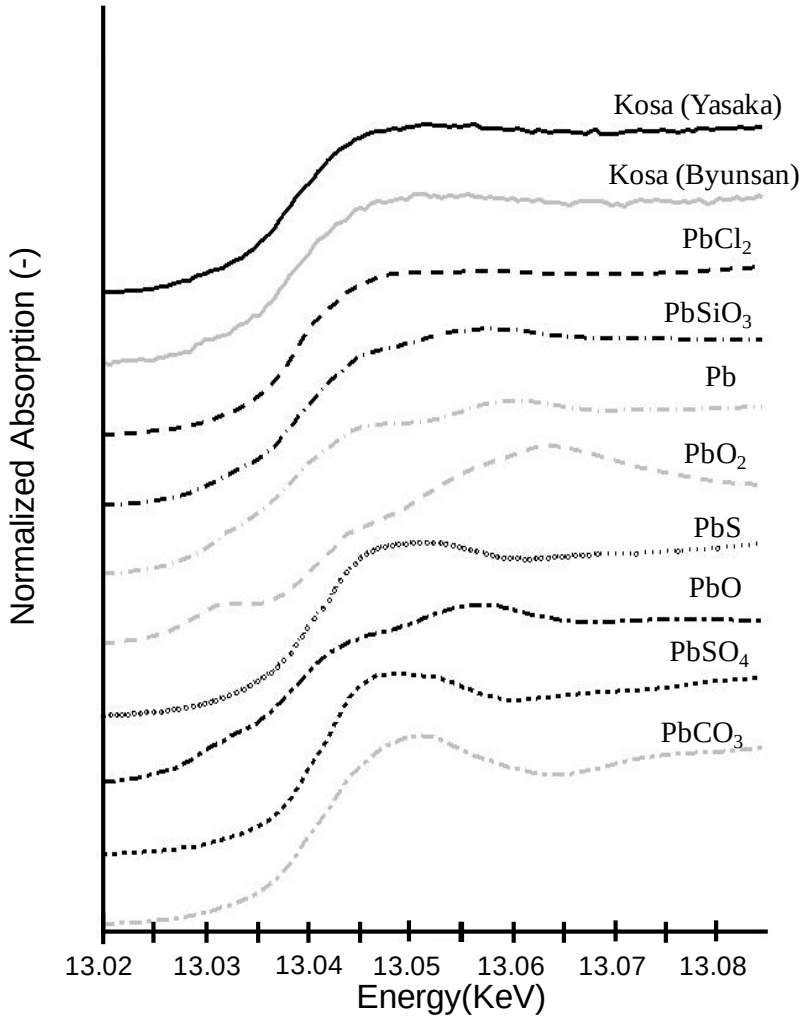

Fig. 12. Pb L3 edge XANES spectra of the various reference materials and the two samples collected using high-volume samplers during the *Kosa* event at Yasaka and Byunsan.